Supplementary material

Photo-assisted methanol synthesis via CO_2 reduction under ambient pressure over plasmonic Cu/ZnO catalysts

Zhou-jun Wang, Hui Song, Hong Pang, Yanxiao Ning, Thang Duy Dao, Zhuan Wang, Hailong Chen, Yuxiang Weng, Qiang Fu, Tadaaki Nagao, Yunming Fang* and Jinhua Ye*

Corresponding Authors: Jinhua.YE@nims.go.jp; fangym@mail.buct.edu.cn

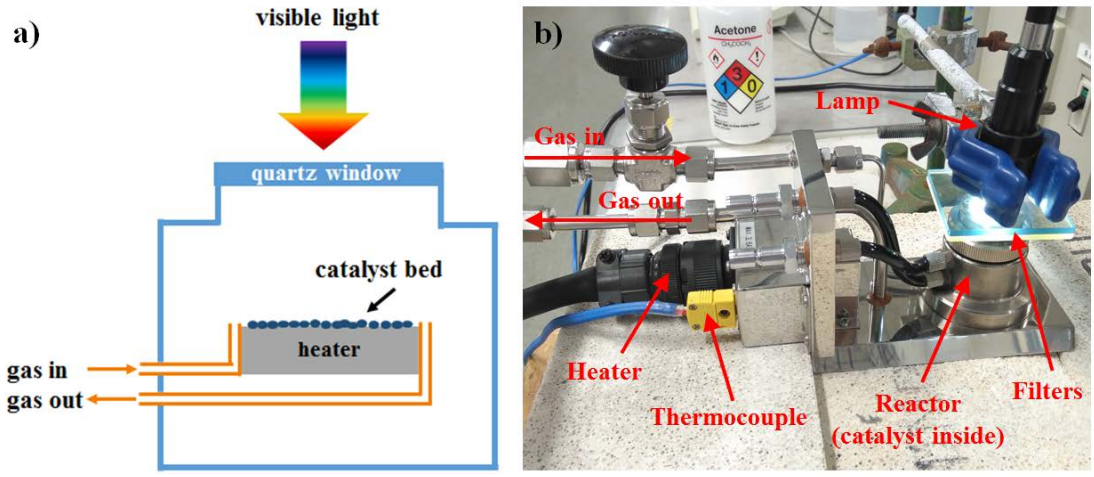

Fig. S1. Schematic of homemade fixed bed reactor (a) and photograph of reaction test setup (b) for photo-thermal catalysis studies.

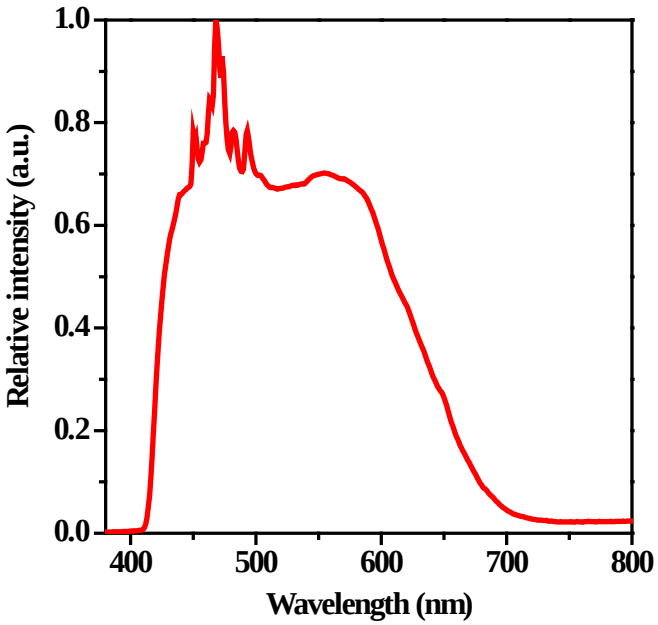

Fig. S2. The spectrum of the visible light source used in the present work.

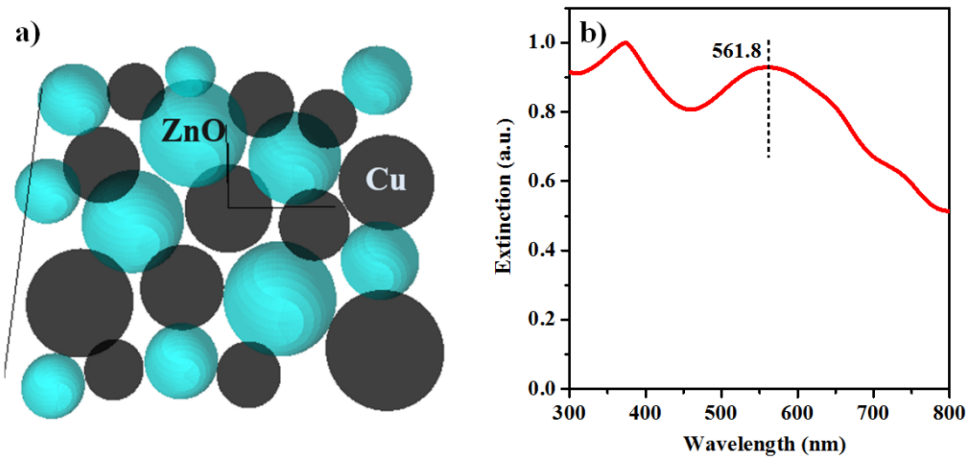

Fig. S3. (a) The model used to simulate the electromagnetic fields of the Cu/ZnO catalyst; (b) The extinction spectrum of the Cu/ZnO catalyst derived from the FDTD simulation, which was consistent with the UV-vis spectrum in Fig. 2a. This consistence suggested that the built model was suitable for the simulation of the electromagnetic fields. The difference between the experimental and simulated peak position of LSPR was mainly due to the disparity in the distribution of size/shape between the model and the actual sample.

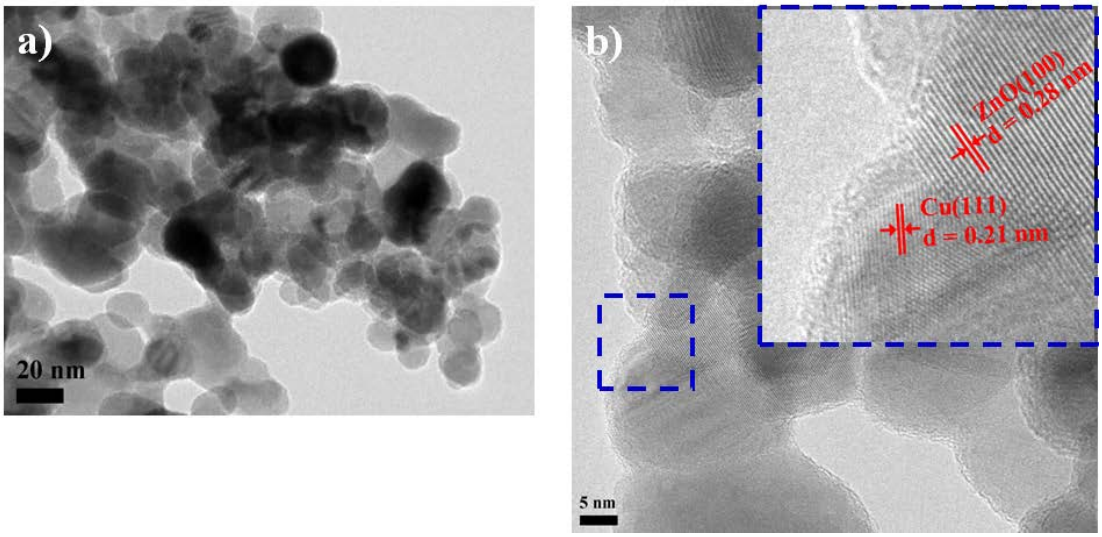

Fig. S4. TEM (a) and HR-TEM (b) images of the reduced Cu/ZnO catalyst. The inset in (b) shows the distance between lattice fringes which was used to identify Cu and ZnO nanoparticles.

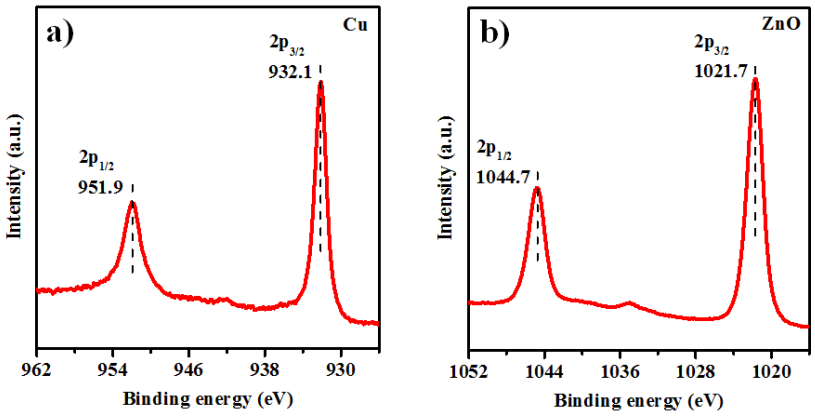

Fig. S5. Cu 2p (a) and Zn 2p (b) XPS spectra of the reduced Cu/ZnO catalyst.

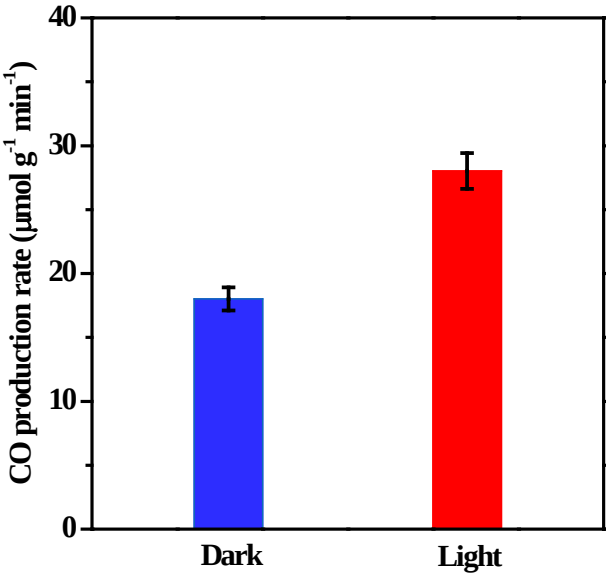

Fig. S6. CO production rate at 220 °C over the Cu/ZnO catalyst with and without visible light irradiation.

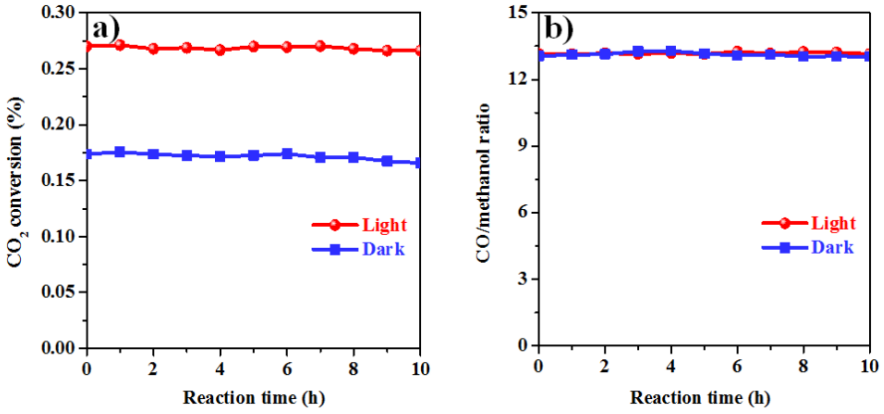

Fig. S7. CO_2 conversion (a) and methanol selectivity (b) as a function of time over the Cu/ZnO catalyst at 220 ºC under dark and light conditions. Methanol selectivity was described with CO/methanol ratio.

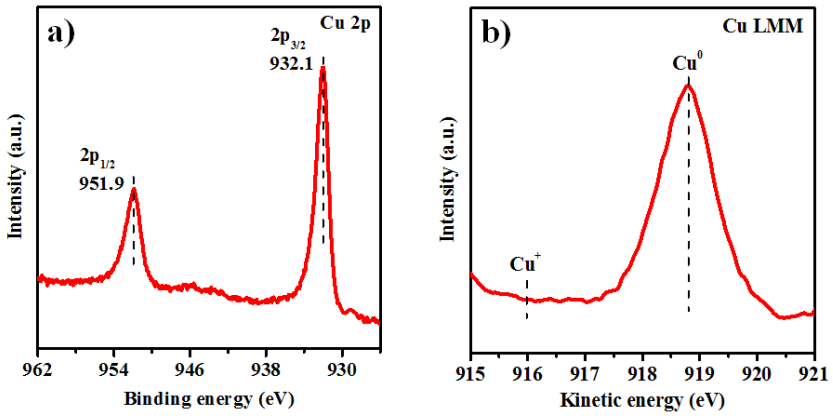

Fig. S8. XPS (a) and AES (b) spectra of Cu species after stability test under dark condition.

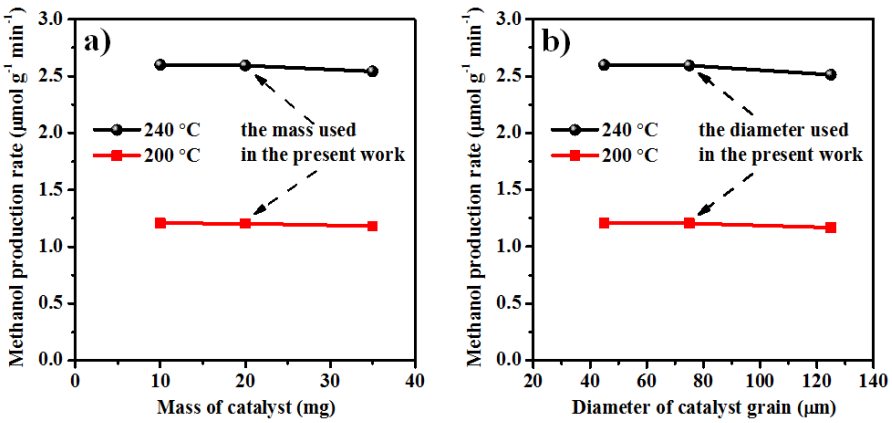

Fig. S9. Examination of the effect of external diffusion (a) and internal diffusion (b) over the Cu/ZnO catalyst at 240 and 200 °C under light condition. The external diffusion was examined by changing the mass of catalyst at a fixed weight hourly space velocity (WHSV = 60 000 ml h^{-1} $gcat^{-1}$). The internal diffusion was examined by changing the diameter of catalyst grain with other reaction conditions fixed.

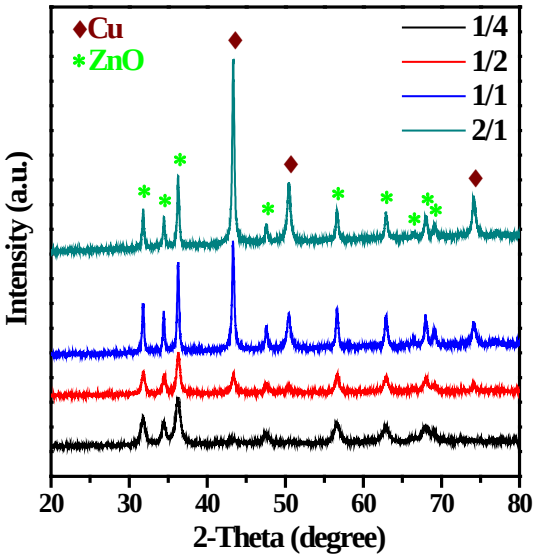

Fig. S10. XRD patterns of Cu/ZnO catalysts with various Cu/Zn molar ratios.

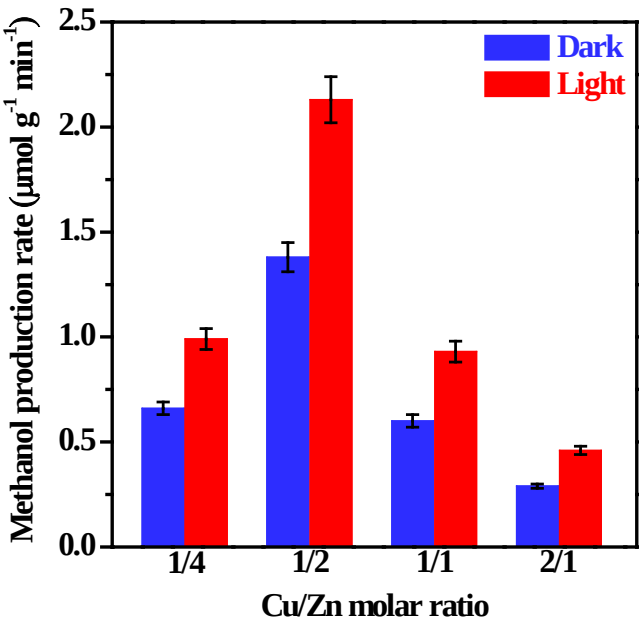

Fig. S11. Methanol production rate at 220 °C over Cu/ZnO catalysts with various Cu/Zn molar ratios.

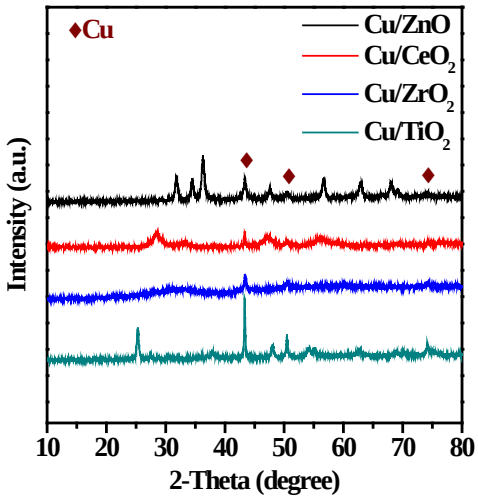

Fig. S12. XRD patterns of Cu catalysts supported on various oxides. The diffraction peaks from the oxide supports were omitted for clearness of Cu features.

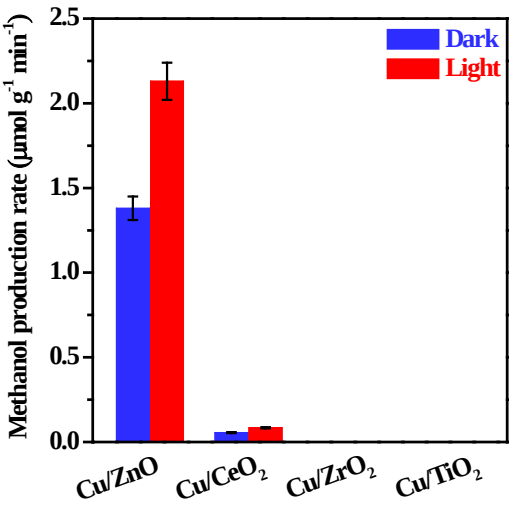

Fig. S13. Methanol production rate at 220 °C under ambient pressure over Cu catalysts supported on various oxides. The methanol produced over Cu/TiO_2 and Cu/ZrO_2 catalysts was below the detection limit under the present reaction conditions.

Table S1. The light intensity distribution among various wavelength ranges.

Wavelength range (nm)	420-480	480-520	520-560	560-600	600-640	640-800
Light intensity ($\mu W\ cm^{-2}$)[a]	13225	115355	114488	120084	80252	48186

[a]The light intensity was measured with a USR-40 spectrophotometer.